Laser-Induced Slip Casting (LIS) – a New Additive Manufacturing Process for Dense Ceramics Demonstrated with Si_3N_4

J. Lüchtenborg[1], T. Mühler[2], F. Léonard[3], J. Günster[*1]

[1]BAM Federal Institute of Materials Research and Testing, Unter den Eichen 87, D-12205 Berlin, Germany, Division 5.4 Ceramic Processing and Biomaterials
[2]Clausthal University of Technology, Zehntnerstrasse 2a, D-38678 Clausthal-Zellerfeld, Germany, Institute of Non-Metallic Materials
[3]BAM Federal Institute of Materials Research and Testing, Berlin, Germany, Division 8.5 Micro Non-Destructive testing

Abstract

Up to now, there exists a lack of methods for the additive manufacturing of voluminous ceramic parts with properties comparable to those of conventionally manufactured ones. A high density after sintering is needed to reach the superior properties of ceramic materials. We have developed a new additive manufacturing method, Laser-Induced Slip casting (LIS), to generate ceramic green bodies with high particle packing density and with virtually no restriction in the particle size of the feedstock, especially in terms of small particles. This is achieved by laser-induced local drying of slurries, with the process resembling many features of the well-established stereolithography, but without the excessive use of polymeric material. Thus, unlike the stereolithography process, the resulting green bodies can be processed like traditionally produced ceramic parts. This method allows large and dense additive-manufactured parts to be obtained from conventional water-based ceramic slurries. As an example, we will demonstrate the application of this novel technique with Si_3N_4.

Keywords: Silicon nitride, additive manufacturing, slurry based

I. Introduction

With minimum lead time and design modifications at the click of a mouse, Additive Manufacturing (AM) is stimulating an entire industry. The material (feedstock) is typically fed into the process as a powder, granulate, paste or suspension, that is the material is in a state optimized for the layer deposition process. In the manufacturing process itself, the material is used to build up the desired object layer by layer and it is simultaneously transferred into a state ideally revealing its final physical properties, or at least a mechanical strength sufficient to transfer the built object to further processing steps. According to the philosophy of AM, the choice of a 3D computer graphic, the 3D model, and material system are sufficient to build a part. Consequently, it is possible to generate parts with arbitrary geometries without the need to adapt the shape to the manufacturing process itself or, vice versa, the process to the shape. Preferably, parts ready to use, i.e. possessing the final physical properties of the desired object, are generated using AM technologies, but also the manufacture of semi-finished parts, requiring additional processing, has turned out to be technically and economically feasible. Most AM technologies that have proven to be commercially viable are based on the processing of polymeric and metallic materials, as they are capable of producing parts with reasonable properties at reasonable costs (e.g. GE's additive-manufactured fuel nozzle [1]). This is mostly based on the fact that fusing or consolidation of polymeric and metallic materials to compact structures in an AM process is much more easily achieved for these classes of materials than for ceramic materials. The reasons for this can be found in the fact that manufacturing of ceramics generally requires the manufacture of powder compacts with high particle packing density prior to their sintering to dense ceramic parts. Moreover, the use of submicron- down to nano-powders is mandatory for the manufacture of most advanced ceramic systems. According to these two requirements, an entire set of technologies has been developed for the AM of ceramics: stereolithography [2, 3, 4], powder-based 3D printing [5, 6, 7], selective laser sintering [8, 9, 10, 11, 12], laminated object manufacturing [13], direct 3D printing [14] and fused deposition modeling [15, 16, 17]. Only a few of these processes are commercially available for the production of ceramics. Moreover, many of them are based on technologies initially designed for polymeric or metallic materials and, merely with adjustment of the feedstock, they have been successfully adapted to ceramic materials. Recently, technologies particularly designed for AM of ceramics have entered the scene, such as slurry-based 3D printing [18] and slurry-based selective laser sintering [19], robocasting [20, 21], and direct ink writing [22, 23]. Their development was triggered by the particular needs for the processing of feedstocks optimized for the manufacture of ceram-

* Corresponding author: jens.guenster@bam.de

ic parts. However, AM of monolithic ceramics enabling the manufactured components to fully retain their superior physico-chemical properties is still a challenge, particularly for voluminous parts. In terms of manufacturing of extremely large parts, AM offers the possibility to significantly reduce costs for the time-consuming and difficult machining of extremely large ceramic parts, green and hard machining. Machining of large ceramic parts can take weeks to a month. Additive manufacturing of ceramic green parts, in combination with additional machining to obtain the desired geometric tolerances, offers a production route alternative to the full machining of isostatic-compacted green bodies. Examples are optical components, camera housings, mirrors and optical benches made from ceramic materials for e.g. the semiconductor industry, military, and aeronautics (Fig. 1).
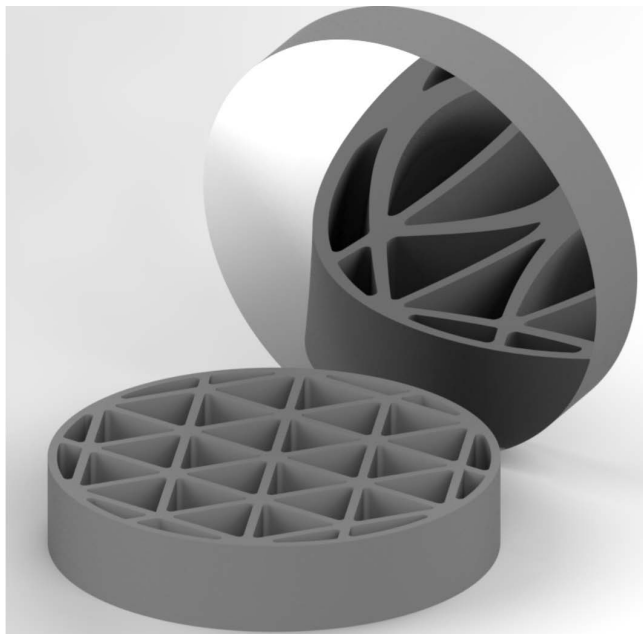

Fig. 1: CAD model of a representative support structure of an optical component with a triangular unit cell.

A major obstacle to the application of additive-manufactured ceramic parts are their mechanical properties, which are very often inferior to those of conventionally manufactured parts. Most of the additive manufacturing processes produce parts with a certain residual porosity [24,25]. Ceramics are very intolerant to flaws like pores because they have a great influence on the ceramics' mechanical properties such as fracture toughness, resulting in potential failure of additive-manufactured parts. Thus, a significant body of literature is devoted to AM of parts in non-load-bearing applications, for example scaffolds in biomedical applications [24], or mechanical properties of porous AM parts are enhanced based on infiltration, for example SiSiC [5]. For additive manufacturing of dense monolithic parts, only a few processes like stereolithography [26] are available. However, stereolithography is limited to parts with small wall thickness owing to the mandatory debinding, which is the thermally induced removal of the organic matrix material in the additive-manufactured ceramic green body. There obviously exists a lack of technologies

for the additive manufacturing of voluminous and dense ceramic parts.

Slurry-based technologies are capable of processing fine or even nano-powders [27]. One of the classical slurry-based processes in ceramic production is slip casting. In slip casting, a porous mold extracts the solvent and, according to its geometry, shapes the green body. One disadvantage of slip casting is the necessity of a mold as this makes small-scale production uneconomic. We bypass this drawback with the new additive manufacturing method Laser Induced Slip casting (LIS). The LIS process additionally offers the opportunity to manufacture more complex parts than possible with slip casting. In the present study, we have used commercial Si_3N_4 slurry to build up voluminous geometries by means of the LIS process.

In the LIS process, the solvent is extracted from the slurry by local evaporation. The local drying of the slurry is induced by intense laser radiation, while the shape of the part is realized by writing the desired geometry in a freshly deposited layer of slurry. With subsequent repetition of the steps layer deposition and laser drying, a part is built (Fig. 2). The formed part is a stable green body, which is immersed in its ceramic slurry during the building process. After extraction from the slurry, the part can be dried and sintered like a green body made by conventional slip casting. The building rate can be varied by the thickness of the deposited layers: Increasing layer thicknesses generally results in higher building rates. Layer thicknesses up to 0.5 mm can be easily realized.

II. Experimental

A silicon nitride slurry is deposited layer by layer with a layer thickness between 200 µm and 500 µm (Fig. 2a). The slurry is fed from a reservoir by a rotary positive-displacement pump, through a gap in an oblong, hollow doctor blade. The slurry is spread by moving the doctor blade at a constant distance parallel to the supporting platform surface. The layer thickness is defined as the gap between the blade and the slurry pool surface. Some excess material is required during the spreading process to allow the process to run without precise control of the feed material volume. Excess slurry is simply pushed over the edge of the vat by the moving blade. A laser system (SPI, 1070 nm wavelength) is used as the energy source for local heating of the slurry. The laser energy is mostly absorbed by the ceramic material in the slurry. In the heated spot, the solvent evaporates and a green body, surrounded by liquid slurry, is generated (Fig. 2b). After laser drying of the desired geometry of one layer, the next layer of slurry is deposited to the vat (Fig. 2c) and locally dried by laser irradiation (Fig. 2d). The repetition of layer deposition and subsequent local drying creates a green body with the desired geometry (Fig. 2e). When the build-up process is finished, the slurry is released from the system and the part can be extracted (Fig. 2f), typically followed by a drying and sintering step. Since a conventional slip-casting slurry is used, it contains only little binder and the green bodies can be sintered with application of a standard sintering schedule. The silicon nitride parts were gas-pressure-sintered. Cross-sections of green bodies and sintered parts are examined with light microscope and SEM
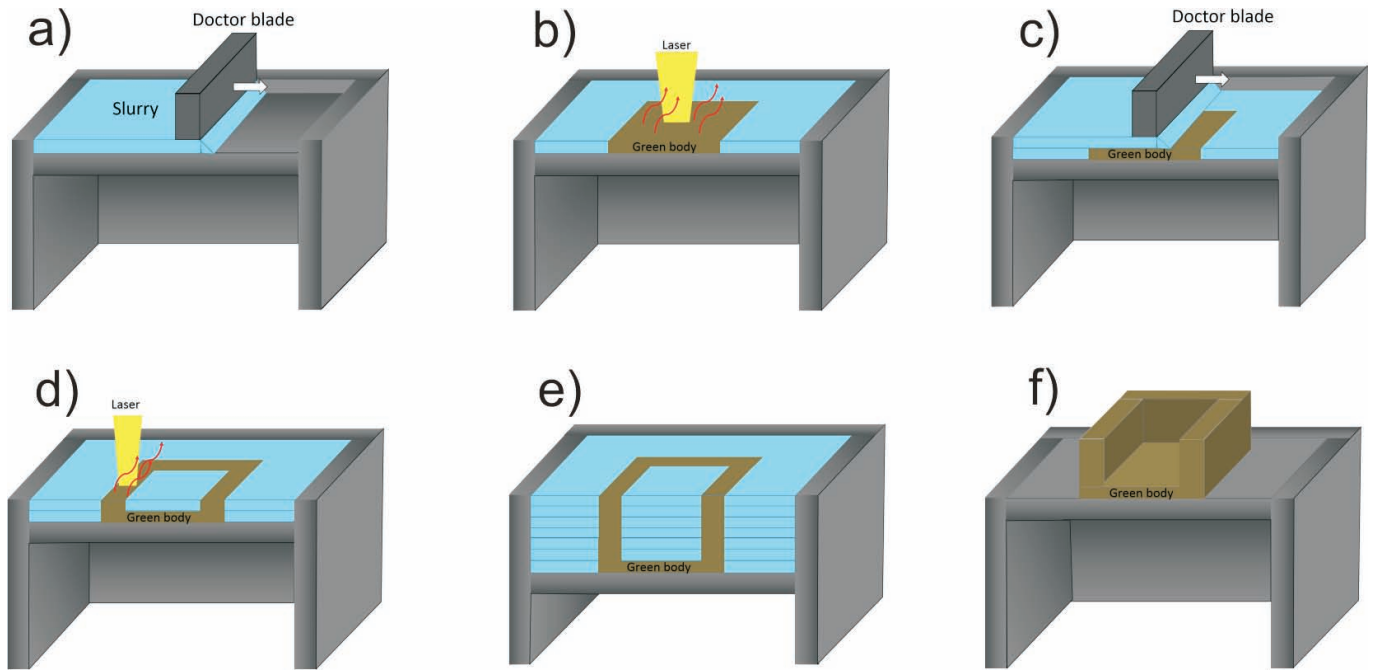
Fig. 2: Illustration of the LIS process: a) A layer of slurry is deposited in the vat. b) A laser locally dries the slurry, creating a green body surrounded by the slurry. c) A new layer of slurry is deposited and subsequently d) the laser locally dries the slurry again. e) A green body with the desired geometry is created. f) The liquid slurry is released from the vat and the free-standing green body remains.

(Zeiss Gemini Supra 40). Mechanical properties of the sintered parts manufactured with Laser Induced Slip casting were characterized in a 4-point bending test. Bending bars, 45 x 4 x 3 mm in size, were prepared from a sintered triangular structure with the bars' long axis prepared parallel to the deposited layers and the layers in plane to the support. 4-point bending tests were conducted with 28 bending bars and analyzed according to Weibull statistics.

Some of the Si_3N_4 parts produced by means of LIS were assessed with X-ray computed tomography (CT). Although CT can simultaneously deliver dimensional measurements and defect detection in 3D, only the latter was performed on a large and small specimen. The scanning was performed on a General Electrics 180/300 kV VTomeX system. For the large specimen, a high-power reflection target 300 kV source was employed. The scanning parameters applied were a voltage of 200 kV, a current of 100 µA, and a filter of 0.25 mm of copper. A series of 3142 projections with a pixel size of 60 µm were acquired over 360°. Each projection was acquired for 1000 ms, for a total scan time of 1 h 55 min. For the small specimen, a transmission target 180 kV source was used to maintain the spot size smaller than the voxel size. The scanning parameters applied were a voltage of 120 kV, a current of 100 µA without filtering. A series of 2600 projections with a pixel size of 3.8 µm was acquired over 360°. Each projection was acquired for 750 ms, for a total scan time of 1 h 14min. The data were reconstructed using General Electrics' proprietary software Phoenix datos x 2 recon. The visualization and data processing were performed using Avizo version 9.0 from FEI.

III. Results

With the Laser Induced Slip casting (LIS) process, silicon nitride ceramic parts have been produced (images of rep-

resentative parts in Fig. 3 and Fig. 4). In the LIS process a ceramic slurry is locally dried and a ceramic green body is formed. The green body does not dissolve in the ambient liquid slurry and can be extracted from the vat after removal of excess slurry. Formation of stable green bodies within the slurry is the result of an irreversible attractive interaction of the ceramics particles, as the particles approach each other during desiccation. Green bodies and subsequently sintered parts of different size and complexity have been produced with silicon nitride slurry. In Fig. 3, two parts manufactured with the LIS process, with the geometry of the basis unit of a rear structure of an optical component after the post sintering process are depicted.
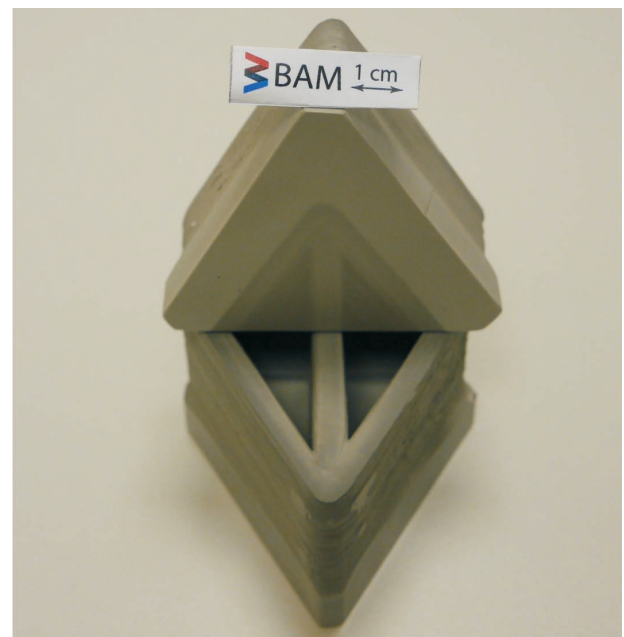
Fig. 3: Two sintered Si_3N_4 parts on top of each other produced with the LIS process.

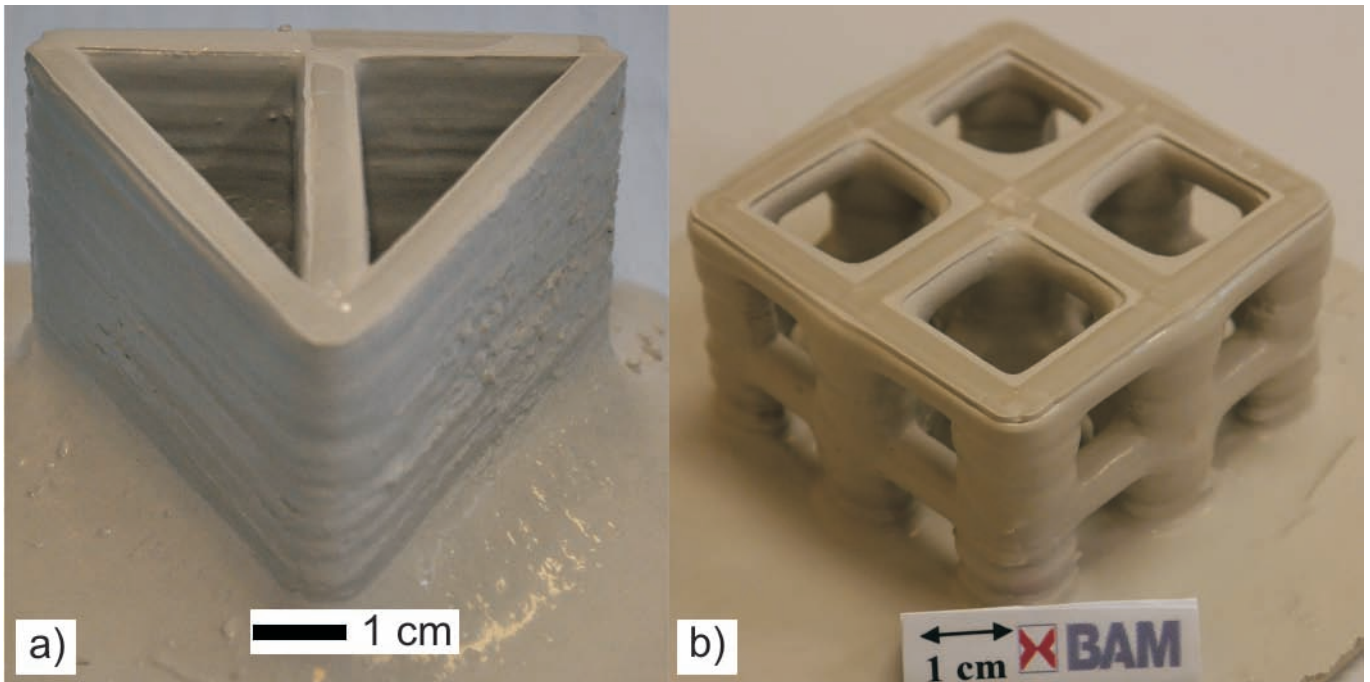**Fig. 4:** Si_3N_4 green body generated by the LIS process. The green body in a) consists of 150 layers with a thickness of 400 µm each. The edge of the triangle has a length of 80 mm. The green body in b) is a structure to demonstrate the possibility to manufacture overhangs.

A green body produced by means of LIS with a triangular structure is shown in Fig. 4a. The presented part has a length of 80 mm along the triangular wall, a height of approximately 50 mm and a wall thickness of 6 mm (Fig. 4a). The object was manufactured by depositing 150 layers of silicon nitride slurry. The building rate in the experimental set-up was approximately 11 cm^3/h, a laser with a maximum power output of 200 W being employed. The inner edges of the triangle are clear and sharp, however, during the production process the formation of a hump at the base of the walls was observed. The surface structure of the walls is smooth, revealing some minor steps oriented parallel to the deposited layers. Besides the triangular structure shown in Fig. 4a, a more complex shape has been built up (Fig. 4b). The structure of the green body consists of two frames connected with pillars. This geometry was designed to demonstrate the possibility to realize overhangs with the LIS process. The dimension of the frames is 45 x 45 mm. The overhangs are 10 mm wide with a height of 10 mm. The overhangs are straight and show no sagging. The walls of the pillars are a little corrugated as a result of a varying layer thickness of deposited layers.

Since the LIS process is, like most additive manufacturing processes, a layer-by-layer process, the interfaces between the layers must be studied carefully. The green bodies and sintered parts were characterized by means of µCT and optical microscopy. The density of the green body generated by the process is 58 % TD. A cross-section of the green body was characterized with optical microscopy. Images are shown in Fig. 5

In optical microscopy, some cross-sections of the green body do not reveal any feature of a layered structure and the green body is dense (Fig. 5a), but predominantly a layered structure of the green body can be recognized (Fig. 5b). The thickness of the layers is not constant for each layer. It varies between 200 µm and 500 µm. Some-

times large pores with a diameter up to 500 µm are visible. They are located at the interface between layers and are of nearly hemispherical shape. A closer look with SEM reveals a dense green body with a well-connected interface between two layers (dashed line Fig. 5c). An interface with inhomogeneities is shown in (Fig. 5d). The lower layer (Layer 2) has a sharp surface and the upper layer (Layer 1) is not attached to the underlying layer. Small cavities with a height of 2 µm and a length up to 10 µm can be seen at the interface.

In a second step, green bodies made with LIS were sintered and characterized by means of optical microscopy, SEM and µCT. For microstructure analysis, cross-sections of the sintered silicon nitride green bodies were investigated: Comparable to the green body, cross-sections with no obvious features of a layered structure and areas with visible interfaces do exist. For a closer investigation of areas with visible interfaces, SEM was used (Fig. 6). SEM images show that the microstructure of the layers looks homogeneous. An interface with a visible gap between two layers is shown in Fig. 6a. The distance between the layers is between 4 and 10 µm. Si_3N_4 crystals have grown into the gap. In Fig. 6b, an interface with minor inhomogeneities is depicted. Pores are aligned next to each other. The larger pore has a length of 10 µm and width of 4 µm. This pore is followed by smaller pores in the area of the interface.

To determine density and local pore distribution, sintered parts were characterized by means of µCT as shown in Fig. 7 and Fig. 8. The red color in the images indicates the flaws in the sample. Fig. 7 shows the µCT scan of an entire sample and Fig. 8 shows the µCT scan with higher resolution of a bending bar prepared from a sintered sample. In the µCT scan of an entire sample (Fig. 7), the distribution of the flaws in the sample is shown. Two observations are relevant: First, pores with a hemispherical
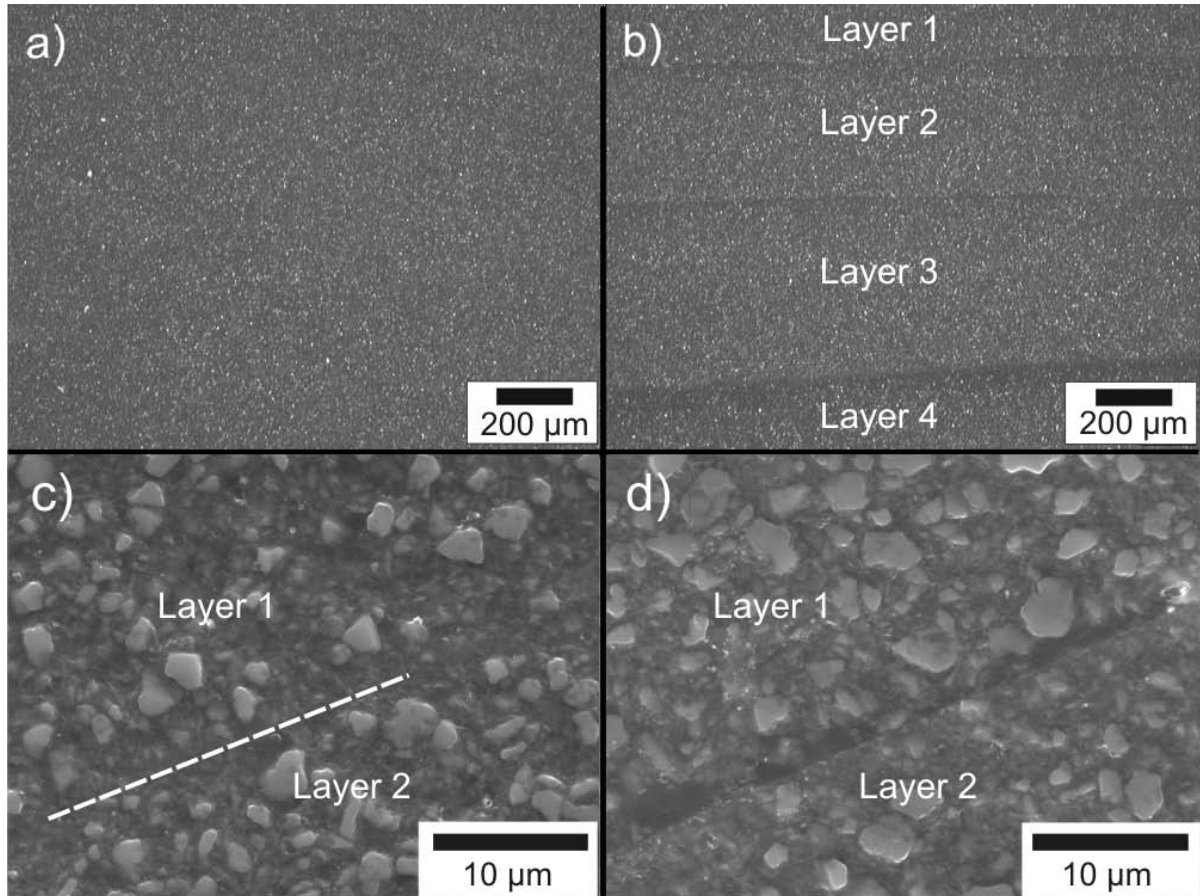
Fig. 5: Optical microscopy images a) and b) and SEM image c) and d), of the cross-section of a green body. a) shows an area where no layer interfaces are visible. b) to d) shows areas with visible layer interfaces, c) good attachment between the two layers at the interface (dashed line), d) elongated cavity at the interface between two layers.
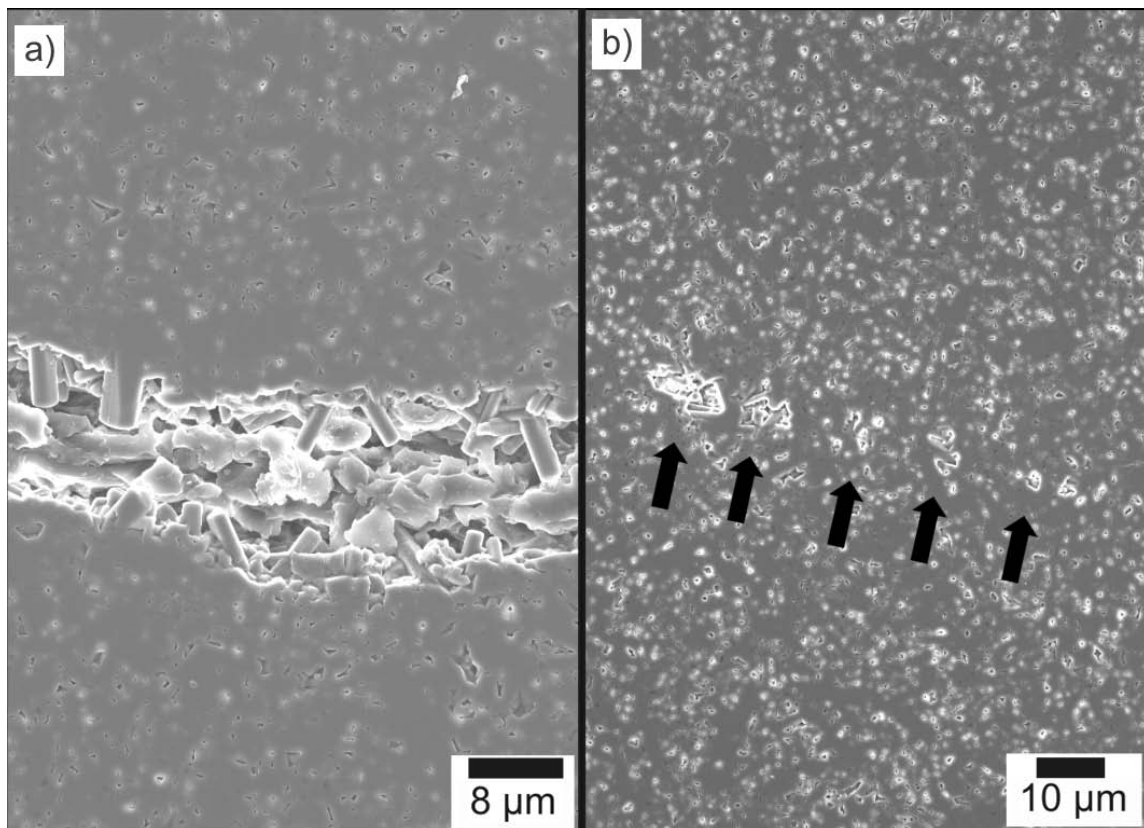

Fig. 6: SEM image of the different visible interfaces between two layers of the sintered Si$_3$N$_4$ sample.

shape are visible. These pores can have a diameter up to 420 µm and are attached to the interface between the layers with the flat part of the pore facing downwards. Furthermore, smaller pores are visible. Second, larger flat areas of flaws are visible. These delaminations or cracks are located parallel to each other and parallel to the layers. The porosity of the part was calculated to 0.41 ± 0.47 %.
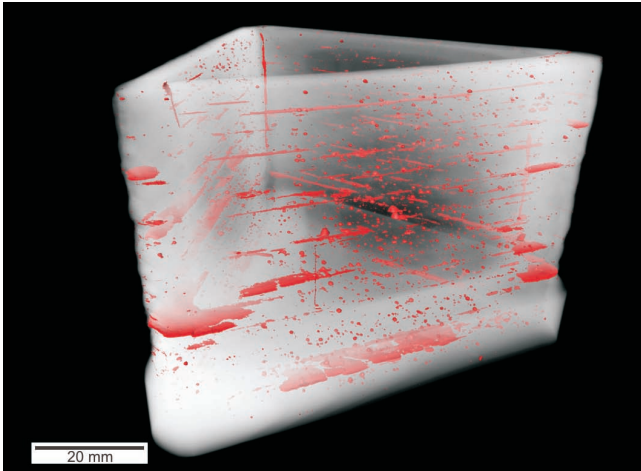

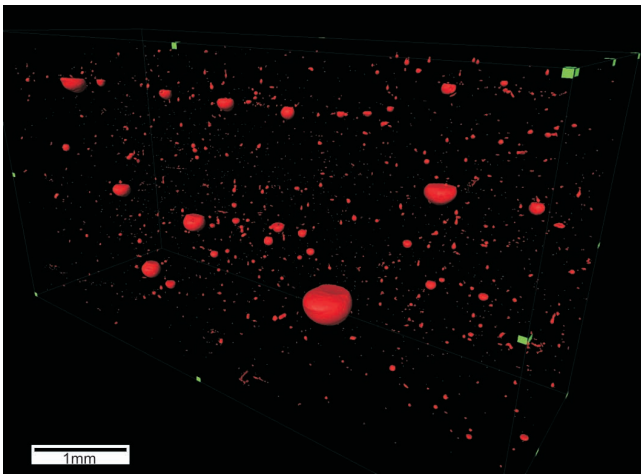**Fig. 7:** µCT reconstruction of a scan of a whole sample. The red color indicates flaws.

Fig. 8: µCT reconstruction of a part of a bending bar. The red color indicates flaws.

In Fig. 8, the flaws in the bending bar are detected. The green color indicates the limits of the reconstructed volume. The image is tilted 180°, that means bottom up, to see the flat side of the hemispherical pores. Large and small pores are visible. The largest pore has a diameter of 420 µm.

Mechanical properties

Mechanical properties of the sintered parts manufactured with Laser Induced Slip casting were characterized in a 4-point bending test. The Weibull parameter m is 4.3 and the mean chracteristic strength σ_0 is 275 MPa. The 28 bending bars were cut out of three different triangular parts. In Fig. 9, the failure probability is plotted versus the flexural strength σ. Nine to ten bending bars were prepared out of each part. Density, Weibull modulus m and characteristic strength σ_0 for the different parts are summarized

in Table 1. The Weibull modulus m and the characteristic strength increase with higher density from $m = 4.0$ and $\sigma_0 = 233$ MPa for the part with a density of 3.15 ± 0.1 g/cm^3 to $m = 6.0$ and $\sigma_0 = 323$ MPa for the part with a density of 3.19 ± 0.1 g/cm^3.

Table 1: Density. Weibull modulus and characteristic strength of the sintered parts.

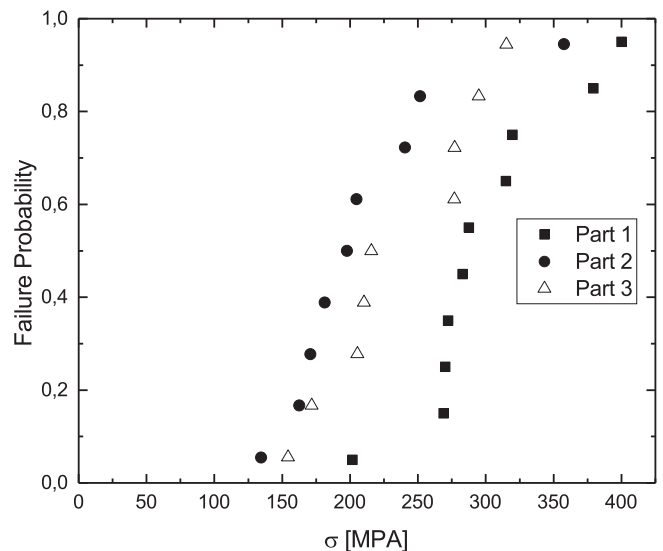| Part	Density (g/cm^3)	Weibull modulus m	Characteristic strength σ_0 (MPa)
Overall	3.17 ± 0.2	4.2	275
1	3.15 ± 0.1	4.0	233
2	3.17 ± 0.1	4.7	258
3	3.19 ± 0.1	6.0	323

Fig. 9: Weibull plot of the Si_3N_4 manufactured with LIS (Part 1 – 3).

The fracture surface of two 4-point bending bars is depicted in Fig. 10. The fracture surface of Fig. 10a reveals a layered structure of the sample. Interfaces between the layers are visible. The flexural strength of this sample is 172.8 MPa. The bending bar in Fig. 10b shows no visible layers. On the upper right edge of the sample, a defect is visible. The flexural strength of sample is 319.7 MPa.

IV. Discussion

The Laser Induced Slip casting (LIS) process opens the possibility to produce ceramic green bodies from slurries with a low amount of or even no organic additives. Test geometries prepared from Si_3N_4 slurry were built to show the possibility to produce large and voluminous ceramic parts. High wall thicknesses, compared to stereolithography, are achievable with LIS.

To demonstrate the technology, the base geometry of a supporting structure of an optical component (Fig. 1) was manufactured out of silicon nitride. This triangular shape geometry with an additional wall in the middle in
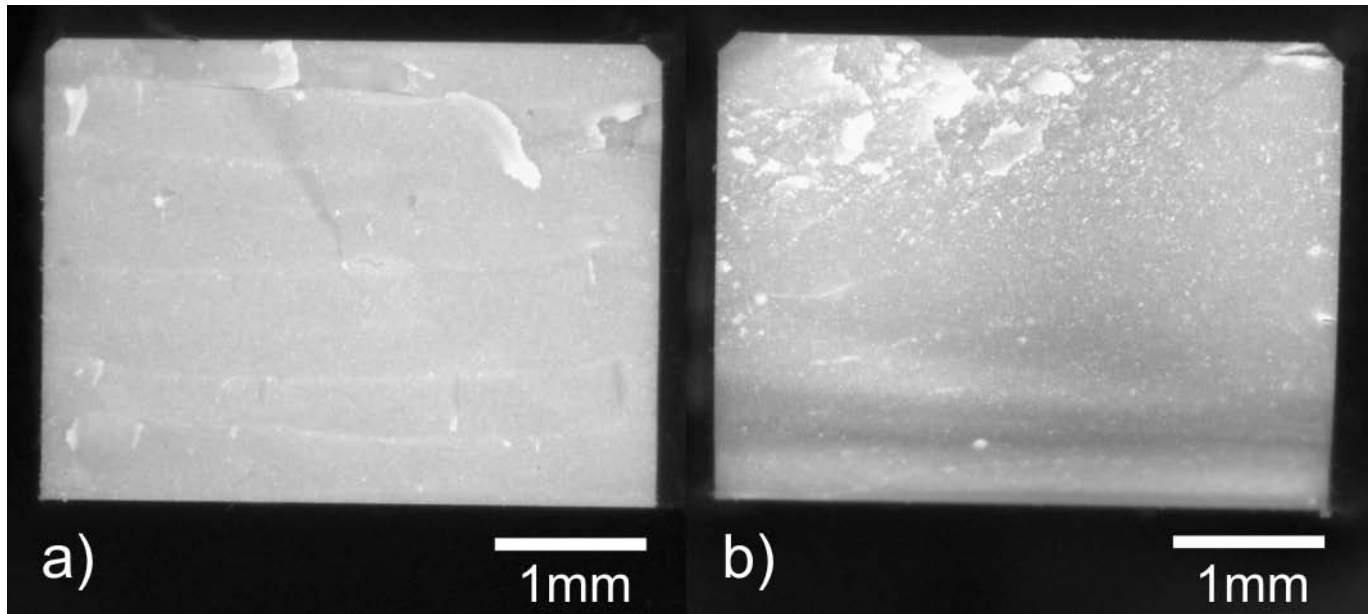
Fig. 10: Fracture surface of two different 4-point bending bars. In a) the layered structure of the sample is visible. In b) no layered structure is visible.

Fig. 4a usually poses problems for conventional manufacturing methods. For example, with slip casting it is generally not possible to produce such geometry because of the free-standing wall and the impossibility to demold. Such geometries are manufactured by machining the structure from an isostatic-pressed body. However, with Laser Induced Slip casting it is possible to generate such geometries. The size of the produced part is only limited by the size of the deposition platform. The building rate in this experimental set-up was 11 cm³/h, which is satisfactory for additive manufacturing of ceramics but too low for an efficient production of large and voluminous ceramic parts. The build-up rate is expected to be much higher when more powerful lasers are employed.

The precision of the manufactured parts is one criterion for the quality of a process. Since this process aims at large and voluminous parts, even an additional post machining for higher-precision parts would be economically feasible. The walls of the parts are smooth but they show some minor steps. The steps are a result of a varying thickness of the deposited layers. Layer deposition was achieved by dosing the slurry through a hollow oblong blade used as a wiper to overcome the surface tension of the slurry and to obtain a smooth surface of the slurry in the vat. The amount of slurry dosed could be reproduced very well, but a dose on demand was not feasible. Hence, excess amount of slurry was dosed and pushed over the edge of the vat by the moving blade. Obviously, a certain amount of slurry could pass in the vat beneath the blade resulting in a slightly thicker layer. As this process is not very reproducible, it results in a varying layer thickness, which, in turn, leads to different widths of the laser path on the slurry surface. In an improved setup, slurry dosing will be on demand, ensuring a constant layer thickness. Furthermore, the formation of a hump at the base of the walls is observed. This hump formation most likely results from an enhanced cast formation in the first layers.

To demonstrate the geometrical flexibility of the Laser Induced Slip casting technology, a structure with overhangs was manufactured (Fig. 4b). Structures with overhangs are generally difficult to generate in vat technologies, such as LIS and stereolithography, as the liquid feedstock does not provide sufficient support. The maximal size of an overhang is limited by two factors: first, the slurry must support the overhang so that this does not sink into the liquid slurry and, second, the overhang, which initially has only the height of one layer, has to have sufficient mechanical strength to survive the deposition of the next layer. Gravitational forces are mostly compensated by the buoyancy in the high-solid-loaded slurry. Fig. 4b demonstrates that it is basically possible to create complex structures with overhangs by means of LIS. Obviously, the relatively high thickness of the first layer forming the overhang, that is 400 µm, provides sufficient strength of the green body for fixation of the overhang in the slurry to withstand forces imposed by the movement of the blade during layer deposition. The LIS process has many similarities to stereolithography concerning the freedom in design, because support of large overhangs by the slurry is rather limited. Nonetheless, higher layer thicknesses enable larger overhangs. The major advantage of the LIS process is, however, the usage of slurries with no or little content of organic additives. Therefore, a standard sintering schedule can be applied to green bodies built up with LIS. Moreover, there are no restrictions in terms of wall thickness and volume of single geometric features imposed, which is strictly not the case for the stereolithography process. Parts produced with stereolithography require time-consuming thermal debinding, which restricts the dimension of monolithic features.

Optical microscopy and SEM of the green bodies and the sintered parts as well as µCT measurements reveal the microstructure of the parts. It is possible to produce dense ceramic parts with additive manufacturing by means of laser-induced local drying. The density of the green body was

estimated to 58 % TD and the sintered parts have a porosity lower than 1 %. With µCT, the porosity was calculated to 0.41 % ± 0.47 % and density values with Archimedes method show a density of 99.4 % TD. The parts produced with LIS show in some areas a microstructure that differs from slip-cast parts. Since LIS is, like most additive manufacturing processes, a layerwise process, interfaces between the layers are visible in some, but not all areas of the green body (Fig. 5) as well as the sintered parts (Fig. 6 and Fig. 10). Generally, layerwise processes are associated with the risk of flaws being generated at the interfaces of the parts. Optical microscope and µCT showed different types of flaws in parts created with the LIS process. Hemispherical-shaped pores are visible (Fig. 8) which can have a diameter up to 420 µm. These pores result from air bubbles in the slurry. The hemispherical shape of the pores is indicative of their origin from bubbles trapped at the surface of a dried layer when a new layer is deposited. The

bubbles get covered with slurry and form pores when the slurry is dried and sintered. Since the air bubble sticks to the surface, the pore develops the hemispherical-shaped geometry. This type of pore is not intrinsic to the process. Another type of flaw are delaminations or cracks, as can be seen as colored areas in the µCT reconstruction in Fig. 7. The cracks form during drying of the wet green bodies. This is common for parts with high wall thickness when these are not dried in a well-defined environment with regard to temperature and humidity. Delaminations could have formed because of the growth mechanism from top to bottom of each layer. The generation of flaws can be explained by a model for the growth of layers:

Model

For the generation of the green body, a defocused laser beam is used as an energy source for local desiccation and consolidation of the slurry layer (see Fig. 11). Depending
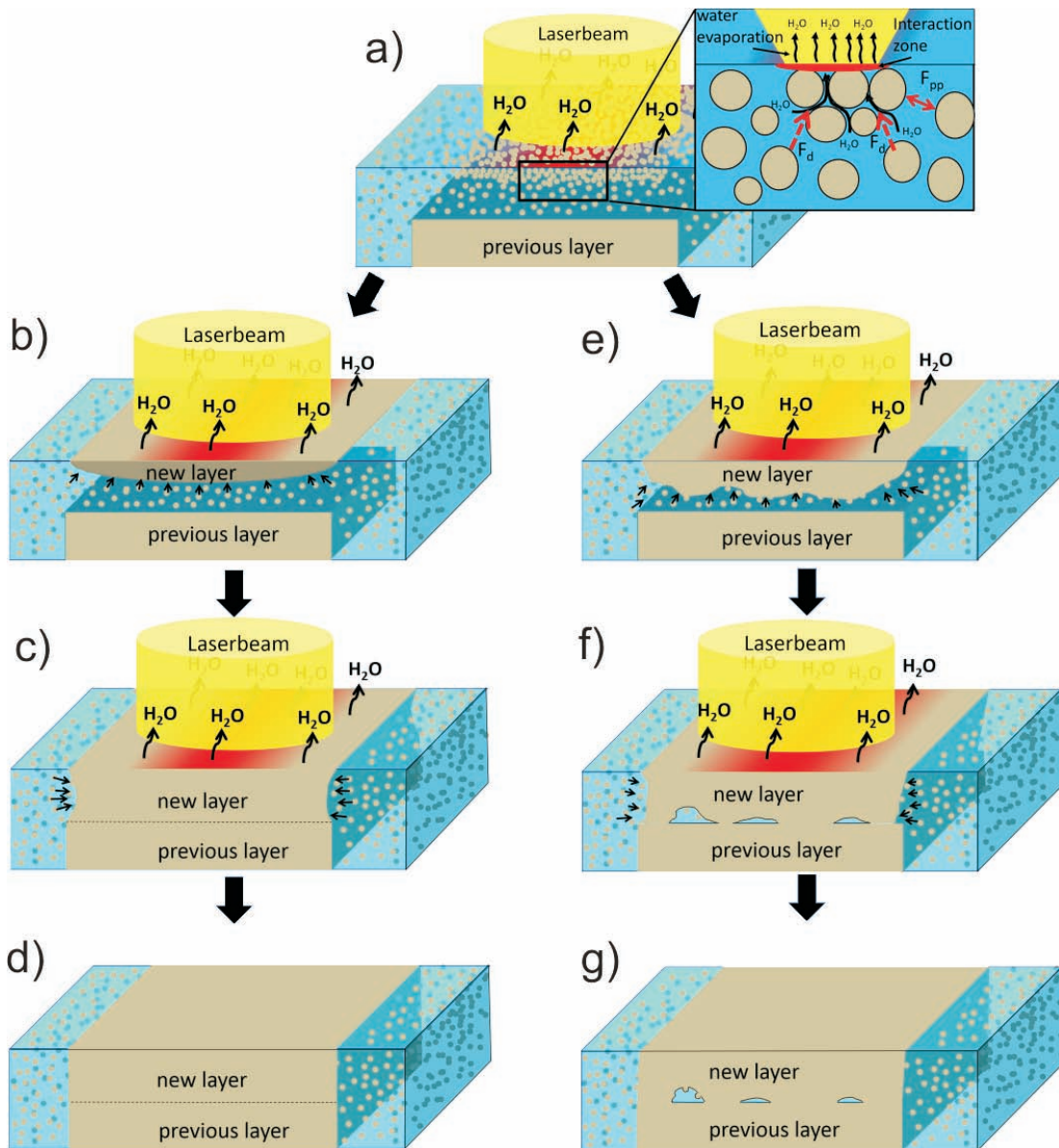
Fig. 11 : Model scenario illustration the LIS process. a) to e) for a uniform naturally slightly convex solidification front of the freshly solidifying layer. a) The laser evaporates water. Due to the created drag force F_d, the particles agglomerate and start forming a solid structure. The layer grows from top to bottom into the slurry until it touches the previous layer. In the case of a uniform solidification front, as illustrated in b) to d), the interface will be good. In the case of a non-uniform solidification front, as illustrated in e) to f), cavities may develop.

on solvent, ceramic powder and wavelength of the laser light, evaporation of the solvent is initiated by directly energy absorption of the solvent or by heating up the powder particles, which in turn heat up the solvent. The solvent, which is water, starts to evaporate (Fig. 11a). Since the laser heats up the surface of the slurry pool, the evaporated water can escape easily. The successive evaporation of water creates a drag force F_d acting on the particles as a result of a flow field of the liquid medium. Like when a mold draws the water out of a ceramic slurry in a slip-casting process, a cast is formed. The particles in the slurry start to agglomerate when the initially repulsive particle-particle force F_{pp} in the slurry disappears and turns into an attractive force as a result of desiccation. A solid layer is formed at the surface of the slurry (Fig. 11a). When the laser treatment continues, more water is evaporated and the layer starts growing from top to bottom into the slurry until it reaches the previously generated solid and connects to it. In this scenario, the shape of the solidification front growing into the slurry deserves a closer look, see also Fig. 11. Figs. 11a to d illustrate the process with a slightly convex but smooth solidification front growing uniformly into the slurry and finally attaching to the previously solidified layer. The layers form a defect-free interface, resembling the situation as observed in Fig. 5d. In Figs. 11e to f the process with a non-uniform solidification front can be seen. For example, inhomogeneous illumination can cause spots where the slurry dries faster, therefore reaching earlier the underlying and previously solidified layer (Fig. 11f). Cavities full of slurry can develop. These cavities are not connected to the outer slurry reservoir and no further slurry can flow in this cavity. During drying, the solvent of the slurry is extracted by the surrounding green body. Since no additional slurry can flow into the cavity at the interface between the two layers, the density of the green body will be decreased or even pores can develop (Fig. 11 g), resembling the situation observation in Fig. 5d or Fig. 6b.

Mechanical properties

The relative low characteristic strength of max. 323 MPa, compared to conventionally processed 900 – 1100 MPa [28], can be explained by the residual pores that can be seen in the green body and the sintered parts. According to fracture mechanics, large pores are most relevant. The largest pores in the manufactured parts are a consequence of the basic deposition process and can be minimized with a new set-up that prevents the formation of air bubbles in the slurry. Cracks visible in the sintered parts and already in the green body are a result of a rough drying procedure. The drying of freshly cast green parts is a very critical process step. In the present study, drying has been performed in laboratory ambient conditions. The delaminations can be minimized with better control of the solidification front of the growing layer by means of better illumination.

V. Conclusions

A new slurry-based additive manufacturing process, Laser-Induced Slip casting (LIS), has been introduced. With the LIS process it is possible to obtain dense and relatively large ceramic green bodies from conventional production slurries containing low amounts of organic binders. The LIS process shares many features with the stereolithography process, but instead of locally crosslinking a photosensitive resin, a laser locally desiccates a conventional ceramic slurry as demonstrated with the example of a Si_3N_4 slurry. The process is designed to generate voluminous ceramic parts by means of the layerwise build-up of parts with a layer thickness larger than 0.5 mm. The microstructure of the parts produced with LIS reveals flaws like pores and delaminations. The density after sintering is 99.4 % TD. Mechanical properties of manufactured parts have been determined in a 4-point bending test. The mechanical properties determined in the 4-point bending test (323 MPa) are still inferior to those of conventionally manufactured Si_3N_4 parts, leaving room for optimization of the process.

References

1 Smith, H.: GE Aviation to grow better fuel nozzles using 3D Printing, 2013.

2 Griffith, M.L., Halloran, J.W.: Freeform fabrication of ceramics via stereolithography, *J. Am. Ceram. Soc.,* **79**, [10], 2601 – 08, (1996).

3 Zhou, W.Z., Li, D.C., Wang, H.: A novel aqueous ceramic suspension for ceramic stereolithography, *Rapid Prototyping J.,* **16**, [1], 29 – 35, (2010).

4 Hull, C.W.: Apparatus for production of three-dimensional objects by stereolitography. US Patent Application US4575330 (1984)

5 Schlier, L., Zhang, W., Travitzky, N., Greil, P., Cypris, J., Weclas, M.: Macro-cellular silicon carbide reactors for nonstationary combustion under piston engine-like conditions, *Int. J. Appl. Ceram. Tec.,* **8**, [5], 1237 – 45, (2011).

6 Melcher, R., Martins, S., Travitzky, N., Greil, P.: Fabrication of Al_2O_3-based composites by indirect 3D-printing, *Mater. Lett.,* **60**, [4], 572 – 75, (2006).

7 Sachs, E.M., Haggerty, J.S., Cima, M.J., Williams, P.A.: Three-dimensional printing techniques. US Patent Application US5204055 (1989)

8 Deckard, C.R.: Method and apparatus for producing parts by selective sintering. US Patent Application US4863538 (1986)

9 Bertrand, P., Bayle, F., Combe, C., Goeuriot, P., Smurov, I.: Ceramic components manufacturing by selective laser sintering, *Appl. Surf. Sci.,* **254**, [4], 989 – 92, (2007).

10 Deckers, J., Meyers, S., Kruth, J.P., Vleugels, J.: Direct selective laser sintering/melting of high density alumina powder layers at elevated temperatures, *Physcs. Proc.,* **56**, 117 – 24, (2014).

11 Nelson, J.C., Xue, S., Barlow, J.W., Beaman, J.J., Marcus, H.L., Bourell, D.L.: Model of the selective laser sintering of Bisphenol-a polycarbonate, *Ind. Eng. Chem. Res.,* **32**, [10], 2305 – 17, (1993).

12 Juste, E., Petit, F., Lardot, V., Cambier, F.: Shaping of ceramic parts by selective laser melting of powder bed, *J. Mater. Res.,* **29**, [17], 2086 – 94, (2014).

13 Feygin, M., Pak, S.S.: Laminated object manufacturing apparatus and method. US Patent Application US5876550.

14 Cappi, B., Özkol, E., Ebert, J., Telle, R.: Direct inkjet printing of Si_3N_4: characterization of ink, green bodies and microstructure, *J. Eur. Ceram. Soc.,* **28**, [13], 2625 – 28, (2008).

15 Yang, H.Y., Yang, S.F., Chi, X.P., Evans, J.R.G.: Fine ceramic lattices prepared by extrusion freeforming, *J. Biomed. Mater. Res. B,* **79B**, [1], 116 – 21, (2006).

16 Crump, S.S.: Modeling apparatus for three-dimensional objects. US Patent Application US5340433 (1989)

[17] Jafari, M.A., Han, W., Mohammadi, F., Safari, Danforth, A.S.C., Langrana, N.: A novel system for fused deposition of advanced multiple ceramics, *Rapid Prototyping J.,* **6**, [3], 161–74, (2000).

[18] Zocca, A., Lima, P., Günster, J.: LSD-based 3D printing of alumina ceramics, *J. Ceram. Sci. Tech.,* 8, [1], 141–47, (2017).

[19] Mühler, T., Heinrich, J., Gomes, C.M., Günster, J.: Slurry-based additive manufacturing of ceramics, *Int. J. Appl. Ceram. Tec.,* **12**, [1], 18–25, (2015).

[20] Schlordt, T., Keppner, F., Travitzky, N., Greil, P.: Robocasting of alumina lattice truss structures, *J. Ceram. Sci. Tech.,* 3 [2] 81–88 (2012).

[21] Miranda, P., Saiz, E., Gryn, K., Tomsia, A.P.: Sintering and robocasting of beta-tricalcium phosphate scaffolds for orthopaedic applications, *Acta Biomater.,* **2**, [4], 457–66 (2006).

[22] Zocca, A., Franchin, G., Elsayed, H., Gioffredi, E., Bernardo, E., Colombo, P.: Direct ink writing of a preceramic polymer and fillers to produce hardystonite ($Ca_2ZnSi_2O_7$) bioceramic scaffolds, *J. Am. Ceram. Soc.,* 99, [6], 1960–67, (2016).

[23] Lewis, J.A., Smay, J.E., Stuecker, J., Cesarano, J.: Direct ink writing of three-dimensional ceramic structures, *J. Am. Ceram. Soc.,* **89**, [12], 3599–609, (2006).

[24] Zocca, A., Colombo, P., Gomes, C.M., Günster, J.: Additive manufacturing of Ceramics: issues, potentialities, and opportunities, *J. Am. Ceram. Soc.,* **98**, [7], 1983–2001 (2015).

[25] Deckers, J., Vleugels, J., Kruthl, J.P.: Additive manufacturing of Ceramics: A review, *J. Ceram. Sci. Tech.,* **5**, [4], 245–60, (2014).

[26] Schwentenwein, M., Homa, J.: Additive manufacturing of dense alumina ceramics, *Int. J. Appl. Ceram. Tec.,* **12**, [1], 1–7, (2015).

[27] Lange, F.F.: Powder processing science and technology for increased reliability, *J. Am. Ceram. Soc.,* **72**, [1], 3–15, (1989).

[28] Riley, F.L.: Silicon nitride and related materials, *J. Am. Ceram. Soc.,* **83**, [2], 245–65, (2000)